Electronic Structure of Early Transition-Metal Carbonyls: Gas-Phase Photoelectron Spectroscopy of (η^5-C_5H_5)M(CO)$_4$ (M = V, Nb, Ta)

Dennis L. Lichtenberger,*,† Hua-Jun Fan,† Nadine E. Gruhn,† Thomas E. Bitterwolf,‡ and Skip Gallagher‡

Department of Chemistry, The University of Arizona, Tucson, Arizona 85721-0041, and Department of Chemistry, University of Idaho, Moscow, Idaho 83844-2343

Received November 22, 1999

Gas-phase photoelectron spectroscopy is used to investigate the bonding between early transition metals and carbonyl and cyclopentadienyl ligands for the molecules (η^5-C_5H_4R)M(CO)$_4$ (R = H, M = V, Nb, Ta; R = $SiMe_3$, M = Nb, Ta; R = $COCH_3$, M = Nb). The lowest ionization energy region contains two overlapping ionizations that arise from the two orbitals that are occupied according to the formal d^4 metal configuration. However, the character of these ionizations is dominated by the carbonyls rather than by the metals, as evidenced by the extensive C−O stretching vibrational progressions observed with these ionizations, by the trends in the ionization cross sections between the molecules and with different ionization sources, and by the relative lack of shifts of these ionizations with metal substitution from vanadium to niobium to tantalum or with trimethylsilyl and acetyl substitutions on the cyclopentadienyl. The second group of ionizations for these molecules corresponds to orbitals with predominantly cyclopentadienyl π character that donate to empty metal d orbitals. A much larger shift of these ionizations is observed upon cyclopentadienyl substitution. The molecular structures are sensitive to the electron configurations. Both density functional theory and ab initio calculations reproduce well the geometry of the neutral molecules and also predict the geometry changes upon ionization. The first ionization, which relates to an orbital with the a_1 symmetry of the metal d_{z^2} orbital, is broad due to a substantial geometry change upon removal of an electron from this orbital. The shoulder on the cyclopentadienyl-based ionizations relates to a dynamic Jahn−Teller geometrical distortion. The unusually large metal-to-carbonyl back-bonding observed in these molecules is facilitated by the interligand overlap between the four carbonyls, which substantially stabilizes the appropriate symmetry-adapted carbonyl π* acceptor orbitals. The extensive carbonyl character in the valence electronic structure diminishes any trends in properties with substitutions of the metals down the group or with substitutions on the cyclopentadienyl ring.

Introduction

The recent publication of a new synthesis route[1−3] to CpM(CO)$_4$ molecules (Cp = η^5-cyclopentadienyl, M = V, Nb, Ta) has made detailed spectroscopic studies of these molecules and their derivatives feasible. Previous synthesis of early transition-metal carbonyl molecules either employed harsh reaction conditions or were of very low yield, which made functionalization difficult to access. With the new reagent Na[$M_2(CO)_8(\mu$-$I)_3$], where M is Nb or Ta, an efficient synthesis route to prepare CpM(CO)$_4$ (M = Nb, Ta) and its derivatives has been developed with much less demanding conditions and much higher yields. This new synthesis route enables a detailed experimental study of the electronic structure of these complexes.

Infrared spectroscopic studies[1,2] indicate that the carbonyl stretching frequencies of these molecules do not change greatly upon addition of substituents on the Cp ligand or with change of the metal center. For example, the carbonyl stretching frequencies of CpNb(CO)$_4$, CpTa(CO)$_4$, (η^5-$C_5H_4Si(CH_3)_3$)Nb(CO)$_4$, and (η^5-$C_5H_4Si(CH_3)_3$)Ta(CO)$_4$ are almost the same within experimental uncertainty.[1,2] The insensitivity of the carbonyl stretching frequencies to changes in the metal or to substituents on the ring provoked our interest in studying the factors that control the electron flow upon the substitution on the ring and replacement of the metal center.

In this study we report the gas-phase He I and He II photoelectron spectra of CpM(CO)$_4$ (M = V, Nb, Ta) as well as the derivatives (η^5-$C_5H_4Si(CH_3)_3$)M(CO)$_4$ (M = Nb, Ta) and (η^5-$C_5H_4COCH_3$)Nb(CO)$_4$, which are used

* To whom correspondence should be addressed. E-mail: dlichten@u.arizona.edu. Fax: 520-621-8407.
† The University of Arizona.
‡ University of Idaho.

(1) Bitterwolf, T. E.; Gallagher, S.; Rheingold, A. L.; Yap, G. P. A. *J. Organomet. Chem.* **1997**, *546*, 27−33.
(2) Bitterwolf, T. E.; Gallagher, S.; Bays, J. T.; Scallorn, B.; Rheingold, A. L.; Guzei, I. A.; Liable-Sands, L.; Linehan, J. C. *J. Organomet. Chem.* **1998**, *557*, 77−92.
(3) Gallagher, S. Dissertation, University of Idaho, Moscow, ID 83844, 1997.

10.1021/om990921m CCC: $19.00
Publication on Web 04/20/2000

to study the perturbations of electronic structure caused by chemical substitutions. A survey of the literature reveals that only the photoelectron spectrum of $CpV(CO)_4$ has been reported previously.[4] A different assignment of the first two ionizations of $CpV(CO)_4$ is presented based on higher precision and signal-to-noise data, and also based on comparisons of the He I and He II spectra through the series of related molecules. Theoretical studies at the approximate Fenske−Hall level, density functional level, and Hartree−Fock level are also reported for both the neutral and cationic species. The geometries and electronic structures obtained via theoretical methods are compared with crystallographic and photoelectron results. All of these results indicate the strong influence of carbonyls on the metal centers of these complexes.

Experimental Section

Data Collection. The molecules were synthesized and characterized using published methods.[1−3] Photoelectron spectra were collected using an instrument that features a 36 cm hemispherical analyzer (McPherson) and custom-designed sample cells, excitation source, and detection and control electronics that have been described elsewhere.[5−8] The argon $^2P_{3/2}$ ionization peak at 15.759 eV was used as an internal calibration lock of the absolute ionization energy. The difference between the argon $^2P_{3/2}$ ionization and the methyl iodide $^2E_{1/2}$ ionization at 9.538 eV was used to calibrate the ionization energy scale. He I (21.2 eV) and He II (40.8 eV) valence spectra were collected for all of the molecules. During data collection, the instrument resolution (fwhm of the Ar $^2P_{3/2}$ peak) was 16−18 meV for He I excitation and 20 meV for He II excitation. All samples sublimed cleanly at room temperature with no need for additional heating.

Data Analysis. The ionization intensities were corrected according to the experimentally determined sensitivity of the instrument as a function of electron kinetic energy. Intensity in the He II spectra due to ionization by He II β photons in the source (48.4 eV photon energy, 12% intensity of He II α source) was removed.[9] The vertical dashed lines in the spectra are the actual data points, with the length of the vertical line representing the variance of each data point. The data are represented analytically in terms of asymmetric Gaussian peaks, which are defined by the position, half widths on the high and low binding energy sides (W_H and W_L), and the amplitude. The number of peaks used for a representation was based solely on the profile of a given band.[10] The uncertainty in the relative band areas is on the order of 5% for overlapping peaks and less than 2% for well-separated ionization bands. The confidence of the peak positions was typically ±0.02 eV. Parameters for overlapping bands are interdependent and less certain than those for well-separated bands.

Electronic Structure and Geometry Calculations. Electronic structure calculations were carried out to compare the energies and characters of the orbitals and ion states with the results of the photoelectron experiments and to explore the dependence of the orbital energies on the molecular geometries. Geometries were first optimized by density functional theory using the package ADF 2.3.0[11−14] on an IBM RS/6000 590 computer with 256MB of memory. These calculations were carried out at the LDA (local density approximation) level with $\alpha = 0.7$. Frozen cores (indicated in parentheses) were used with triple-ζ functions for V(3p), Nb(4p), and Ta(5p) (as provided in ADF's standard type-IV basis set) and with double-ζ functions for Si(2p), O(1s), and C(1s) (as provided in ADF's standard type-II basis set). The optimized geometries, which compared well with crystal structures, were then used as the starting point for the subsequent electronic structure calculations in both ab initio and Fenske−Hall methods.

The ab initio calculations were carried out on SGI Origin 2000 computers with 12 GB of memory and 48 processors using the package Gaussian 94, Revision E.2.[15] Visualizations of molecular orbital isosurfaces were produced using VTK[16,17] developed in this laboratory. All of the ab initio calculations used the LANL2DZ ECP basis set, which is the Dunning/Huzinaga full double-ζ basis for the first-row atoms,[18] and the Los Alamos ECP plus DZ on other atoms.[19−21] Geometry optimizations were also carried out with ab initio calculations on both the neutral and the lowest $^2A'$ and $^2A''$ cation species within the restricted Hartree−Fock and unrestricted Hartree−Fock models. Møller−Plesset correlation energy corrections, truncated at second-order (MP2), were also examined.

For investigation of Jahn−Teller effects with ionization from the Cp e_1'' π-based orbitals, the stabilization energy provided by Cp ring distortion in the positive ion was estimated by a series of ab initio Hartree−Fock calculations on $CpNb(CO)_4$. The geometry of the Cp ligand in the $CpNb(CO)_4$ molecule was varied incrementally along a distortion coordinate that is defined as the distortion from the optimized D_{5h} symmetry of free Cp^- with filled e_1'' π orbitals to the optimized C_{2v} geometry of free Cp in the $^2A''$ state that has one electron removed from the e_1'' π orbitals. This distortion is shown amplified by a factor of 10 in Figure 6. The geometry of the $Nb(CO)_4^+$ portion of the molecule was held constant, so the stabilization energy that is obtained is a lower bound to what would be obtained if full optimization of the excited state could be obtained. Unfortunately, the $^2A'$ and $^2A''$ positive ion states of $CpNb(CO)_4$ that correspond to removal of an electron from a Cp-based orbital are excited states, and SCF calculations that start with these states collapse to lower states of these symmetries. Therefore, the energies of the Cp-based positive ions were estimated by the frozen-orbital Koopmans' approximation[22] using the eigenvalues from the neutral-molecule calculations along the distortion coordinate.

(4) Green, J. C. *Struct. Bond.* **1981**, *43*, 37−112.
(5) Lichtenberger, D. L.; Calabro, D. C.; Kellogg, G. E. *Organometallics* **1984**, *3*, 1623.
(6) Calabro, D. C.; Hubbard, J. L.; Blevins, C. H., II; Campbell, A. C.; Lichtenberger, D. L. *J. Am. Chem. Soc.* **1981**, *103*, 6839−6846.
(7) Kellogg, G. *Diss. Abstr. Int. B* **1986**, *46*, 3838; University of Arizona: Tucson, AZ 85721.
(8) Lichtenberger, D. L.; Kellogg, G. E.; Kristofzski, J. G.; Page, D.; Turner, S.; Klinger, G.; Lorenzen, J. *Rev. Sci. Instrum.* **1986**, *57*, 2366.
(9) Renshaw, S. K. *Diss. Abstr. Int. B* **1992**, *51* (10), 5259.
(10) Lichtenberger, D. L.; Copenhaver, A. S. *J. Electron. Spectrosc. Relat. Phenom.* **1990**, *50*, 335−352.
(11) ADF 2.3.0, Theoretical Chemistry; Vrije Universiteit: Amsterdam, The Netherlands.
(12) Baerends, E. J.; Ellis, D. E.; Ros, P. *Chem. Phys.* **1973**, *2*, 41−51.
(13) te Velde, G.; Baerends, E. J. *J. Comput. Phys.* **1992**, *99*, 84−98.
(14) Fonseca Guerra C.; et al. In *Methods and Techniques in Computational Chemistry*; Clementi, E., Corongiu, G., Eds.; STEF: Cagliari, 1995.
(15) Frisch, M. J.; Trucks, G. W.; Schlegel, H. B.; Gill, P. M. W.; Johnson, B. G.; Robb, M. A.; Cheeseman, J. R.; Keith, T. A.; Petersson, G. A.; Montgomery, J. A.; Raghavachari, K.; Al-Laham, M. A.; Zakrzewski, V. G.; Ortiz, J. V.; Foresman, J. B.; Cioslowski, J.; Stefanov, B. B.; Nanayakkara, A.; Challacombe, M.; Peng, C. Y.; Ayala, P. A.; Chen, W.; Wong, M. W.; Andres, J. L.; Replogle, E. S.; Gomperts, R.; Martin, R. L.; Fox, D. J.; Binkley, J. S.; Defrees, D. J.; Baker, J.; Stewart, J. P.; Head-Gordon, M.; Gonzalez, C.; Pople, J. A. *Gaussian 94, Revision E.2*; Gaussian, Inc.: Pittsburgh, PA, 1995.
(16) Uplinger, A. B. *Diss. Abstr. Int. B* **1998**, *59* (5), 2197; University of Arizona: Tucson, AZ 85721.
(17) Schroeder, W.; Martin, K.; Lorensen, B. *The Visualization Toolkit*; Prentice Hall: Upper Saddle River, NJ, 1996.
(18) Dunning, T. H., Jr.; Hay, P. J. In *Modern Theoretical Chemistry*; Schaefer, H. F., III, Ed.; Plenum Press: New York, 1976; Vol. 3, pp 1−27.
(19) Hay, P. J.; Wadt, W. R. *J. Chem. Phys.* **1985**, *82*, 270.
(20) Wadt, W. R.; Hay, P. J. *J. Chem. Phys.* **1985**, *82*, 284.
(21) Hay, P. J.; Wadt, W. R. *J. Chem. Phys.* **1985**, *82*, 299.
(22) Koopmans, T. *Physica* **1933**, *1*, 104.

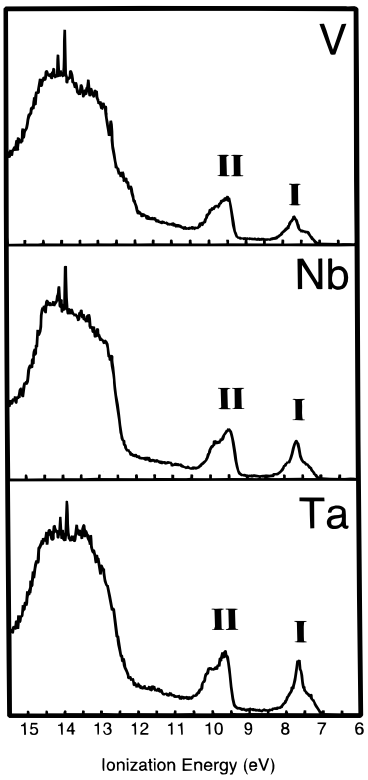

Figure 1. He I photoelectron spectra of (η^5-C_5H_5)M(CO)$_4$ (M = V, Nb, Ta).

Results and Discussion

General Features of the Spectra. The He I spectra of CpM(CO)$_4$ from 5 to 15 eV for M = V, Nb, and Ta are presented in Figure 1. Each spectrum shows three separate regions. The region with ionization energies higher than about 12 eV contains the ionizations from carbon−carbon and carbon−hydrogen σ bonds of the Cp ring, the symmetric π orbital of the Cp ligand (a_2'' in D_{5h} symmetry), and the 5σ and 1π orbitals of the carbonyl ligands. The large degree of overlap among these ionizations precludes obtaining much specific information from this region. In contrast, a large amount of information on the electronic structure of these molecules is available from the ionizations in the two separate regions below 12 eV. Region **I** in the figure, from about 6.5 to 8.5 eV, and region **II**, from about 9 to 11 eV, each contains a distinctive ionization band. The profile of the ionization band in region **II** shows a shoulder on the high ionization energy side in each spectrum. The shape and energy of this ionization band are characteristic of ionizations that originate from predominantly cyclopentadienyl π orbitals (e_1'' in D_{5h} symmetry) in piano stool molecules.[6,23] The ionization band in region **I**, as discussed below, arises from the formally d^4 configuration of the metals, and two ionizations from filled orbitals are expected in this region. The profile of band **I** is more complex, and evaluation of the characteristics of this ionization says much about the electronic structure of these molecules.

An observation that is immediately apparent when looking at Figure 1 is that the ionization features of these molecules are nearly identical despite changing the central metal atom from V to Nb to Ta. The only discernible change is a slight increase in the relative intensity of the first band from the CpV(CO)$_4$ molecule to the CpTa(CO)$_4$ molecule. From the theoretical atomic photoionization cross sections per valence electron[24] in Table 1, ionization of Ta 5d orbital electrons is expected to have three times the probability of ionization of V 3d orbital electrons, but only a small change in the relative intensities of the ionizations in regions **I** and **II** is observed between these spectra. Other than this, the ionization bands are very similar in both band positions and profiles for all three molecules. This is in contrast to the previously observed changes in valence ionizations with metal substitutions in the cyclopentadienyl−carbonyl molecules of later transition metals. For instance, the initial ionizations of CpM(CO)$_3$ molecules are clearly split when Re replaces Mn because of the spin−orbit coupling parameter of Re 5d electrons.[6] No such splitting or even broadening from the spin−orbit coupling parameter of Ta 5d electrons is observed in the ionizations of the CpTa(CO)$_4$ molecule. As another example, the initial ionizations of CpCo(CO)$_2$ and CpRh(CO)$_2$ are greatly different,[23,25,26] but the initial ionizations of CpV(CO)$_4$ and CpNb(CO)$_4$ are nearly identical. This similarity in the ionizations of the V, Nb, and Ta molecules suggests that there is a relatively small amount of metal character associated with the valence ionizations. This point will be probed by a number of techniques. We will begin with a qualitative discussion of the orbital interactions, then examine the ionization profiles in detail, compare the ionization intensities as a function of the ionization source energy and atomic characters, examine the effects of cyclopentadienyl substitutions, and finish with the results of density functional theory and ab initio Hartree−Fock calculations with inclusion of electron correlation.

Table 1. Comparison of Theoretical Atomic Photoionization Cross Sections[24] per Valence Electron of Vanadium, Niobium, Tantalum, Carbon, and Oxygen

atom (orbital)	photoionization cross section (Mbarn)		He II/He I ratio in relation to C
	He I	He II	
V (3d)	1.94	1.98	3.34
Nb (4d)	5.53	1.16	0.69
Ta (5d)	6.15	1.63	0.87
C (2p)	3.04	0.94	1
O (2p)	2.67	1.70	2.09
Si (3p)	0.16	0.16	3.29

Qualitative Considerations. Before discussing the spectra further, it is helpful to consider the general electronic structure of CpM(CO)$_4$ molecules. To illustrate, Figure 2 shows a molecular orbital diagram of CpNb(CO)$_4$ constructed from a Fenske−Hall calculation. The molecular orbital diagrams of V and Ta can be constructed in the same fashion and are similar to the one shown. The coordinates are set up in such a way that the *Z*-axis points from the metal center to the centroid of the Cp ring, and the *XZ*- and *YZ*-planes contain the carbonyls. It should be pointed out that, for

(23) Lichtenberger, D. L.; Calabro, D. C.; Kellogg, G. E. *Organometallics* **1984**, *3*, 1623−1630.

(24) Yeh, J. J.; Lindau, I. *Atom. Data Nucl. Data* **1985**, *32*, 1.
(25) Dudeney, N.; Kirchner, O. N.; Green, J. C.; Maitlis, P. M. *J. Chem. Soc., Dalton Trans.* **1984**, *9*, 1877−1882.
(26) Li, X.; Bancroft, G. M.; Puddephatt, R. J.; Hu, Y.-F.; Tan, K. H. *Organometallics* **1996**, *15*, 2890−2904.

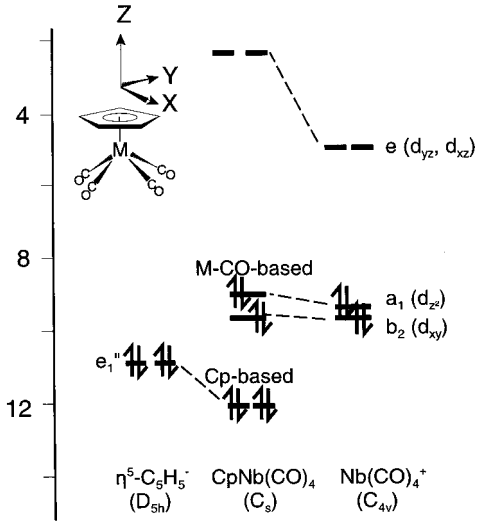

Figure 2. Molecular orbital diagram of (η^5-C_5H_5)Nb(CO)$_4$ constructed from a Fenske−Hall calculation in terms of the η^5-C_5H_5 and Nb(CO)$_4$ fragments.

sake of discussion, the labels of these molecular orbitals are retained from the symmetry labels within each fragment. That is, the top two occupied orbitals of the Cp^- fragment are the e_1'' π orbitals in D_{5h} symmetry. Similarly, the top two occupied orbitals of the M(CO)$_4^+$ fragment are the a_1 and b_2 orbitals in C_{4v} symmetry. Although the whole molecule only has C_s symmetry and the top two orbitals of each fragment are simply a′ and a″, the experiments indicate that the electronic separation and local symmetries of these fragments provide a useful model.

The Fenske−Hall molecular orbital diagram agrees with the ionizations observed in the spectra. For instance, band **I** from 6.5 to 8.5 eV is assigned to ionizations arising from the predominantly metal−carbonyl-based a_1 and b_2 orbitals, and band **II** from 9 to 11 eV is assigned to ionizations arising from the predominantly Cp e_1'' π-based orbitals. Orbital energies are related to the ionization energies via Koopmans' theorem,[22] which ignores the electron relaxation energy and change in correlation energy upon ionization. It is interesting to note that the first four calculated orbital energies scale to the experimental ionization energies with a factor of 0.80 ± 0.02. This scaling factor is typical of the factors that have been found in a number of studies relating the orbital energies from approximate and semiempirical calculations to ionization energies.[27]

The top two filled orbitals of the molecule, the a_1 and b_2, correlate by symmetry with the metal d_{z^2} and d_{xy} orbitals, respectively. These orbitals will occasionally be referred to as the a_1 (d_{z^2}) and the b_2 (d_{xy}) orbitals as a reminder of their origin. The d_{z^2} and d_{xy} are the two metal d orbitals expected to be filled for the d^4 configuration in a simple crystal field analysis, in which the d_{xz}, d_{yz}, and $d_{x^2-y^2}$ orbitals are most directed toward the carbonyls. However, the Fenske−Hall calculation predicts that the a_1 orbital is only 45% metal d_{z^2} character and the b_2 orbital is only 49% metal d_{xy} character. More than half of the character of these two orbitals is on the carbonyl ligands. Strong donation to the four carbonyls is favored by the angular overlaps of the orbitals in the structure of these molecules. According to experimental structural information, the Cp(centroid)−M−CO angle of CpM(CO)$_4$ and other derivative molecules are all close to 120°; for example, (η^5-C_5H_5)Ta(CO)$_4$ is 121.3(7)°,[2] (η^5-$C_5H_4CH{=}CH_2$)Nb(CO)$_4$ is 121(2)°,[28] and (η^5-C_5H_5)V(CO)$_4$ is 120(2)°.[29] At this particular angle both of the filled metal orbitals, the d_{z^2} and d_{xy}, can back-bond to the carbonyls. Notice that the node of the d_{z^2} orbital is near 125°, so the structure is very close to the angle that minimizes the d_{z^2} orbital overlap with carbonyl σ-bonding orbitals and maximizes the overlap with the carbonyl π orbitals. Additional factors that favor back-bonding to the carbonyls in these molecules will be discussed later. The surface plots of the top two orbitals of these molecules from the Fenske−Hall calculations are shown below. The extensive overlap and delocalization of the electron density in these orbitals to all four carbonyls is apparent. For this reason, in the following discussion the ionizations in band **I** will be referred to as the metal−carbonyl-based ionizations instead of the metal-based ionizations, as has been common in previous studies of organometallic molecules.

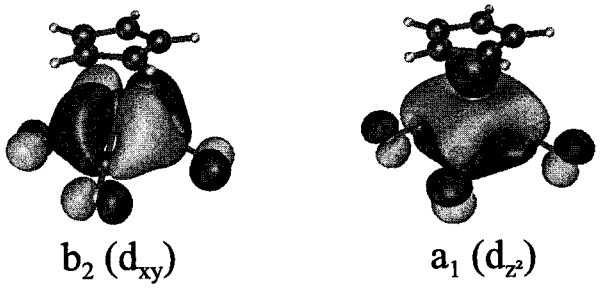

These metal−carbonyl orbitals show little interaction with the cyclopentadienyl orbitals, and this is expected even if the metal−carbonyl orbitals were high in metal character. The metal d_{z^2} orbital, as in ferrocene,[30] has the correct symmetry for interaction with the symmetric cyclopentadienyl π orbital (a_2'' in D_{5h}), but actually has little interaction because the d_{z^2} orbital node is directed toward the Cp π orbital lobes. In addition, the metal d_{z^2} orbital and the Cp a_2'' π orbital are well-separated in energy, which is also unfavorable for interaction. Likewise, the d_{xy} orbital has only a weak δ-type overlap with one of the empty Cp e_2'' π orbitals, and a large energy gap exists between these orbitals, so no strong interaction is expected. According to the Fenske−Hall calculations, the highest occupied a_1 and b_2 orbitals of the Nb(CO)$_4$ fragment remain 98% pure in the CpNb(CO)$_4$ molecule. On the other hand, the cyclopentadienyl e_1'' π ionizations from 9 to 11 eV, which correspond to the third and fourth highest occupied orbitals in Figure 2, are expected to contain some metal character because donation from these Cp orbitals into the empty metal d_{xz} and d_{yz} orbitals is important in forming the M−Cp bond. The stabilization of these orbital energies by mixing with the metal is evident in the energy diagram

(27) Cornil, J.; Vanderdonckt, S.; Lazzaroni, R.; dos Santos, D. A.; Thys, G.; Geise, H. J.; Yu, L.-M.; Szablewski, M.; Bloor, D.; Lögdlund, M.; Salaneck, W. R.; Gruhn, N. E.; Lichtenberger, D. L.; Lee, P. A.; Armstrong, N. R.; Brédas, J. L. *Chem. Mater.* **1999**, *11*, 2436−2443.

(28) Herrmann W. A.; Kalcher W.; Biersack, H.; Bernal, I.; Creswick, M. *Chem. Ber.* **1981**, *114*, 3558−3571.

(29) Almond, M. J.; Page, E. M.; Rice, D. A.; Hagen, K. *J. Organomet. Chem.* **1996**, *511*, 303−307.

(30) Gruhn, N. E.; Lichtenberger, D. L. *Inorg. Electron. Struct. Spectrosc.* **1999**, *2*, 533−574.

Table 2. Energies, Shapes, and Relative Areas of Low-Energy Valence Ionizations

label	position (eV)	W_H (eV)	W_L (eV)	He I peak area	He II peak area	He II/I ratio
			$(\eta^5\text{-}C_5H_5)V(CO)_4$			
a_1 (d_{z^2})	7.41	0.44	0.27	0.59	1.19	2.03
b_2 (d_{xy})	7.71	0.27	0.23			
Cp e_1''	9.47	0.42	0.22	1	1	1
	9.87s[a]	0.49	0.49			
			$(\eta^5\text{-}C_5H_5)Nb(CO)_4$			
a_1 (d_{z^2})	7.41	0.29	0.26	0.59	2.24	3.79
b_2 (d_{xy})	7.67	0.26	0.22			
Cp e_1''	9.47	0.43	0.23	1	1	1
	9.88s	0.43	0.38			
			$(\eta^5\text{-}C_5H_5)Ta(CO)_4$			
a_1 (d_{z^2})	7.40	0.27	0.26	0.75	1.81	2.41
b_2 (d_{xy})	7.65	0.22	0.20			
Cp e_1''	9.62	0.58	0.21	1	1	1
	10.09s	0.41	0.29			
			$(\eta^5\text{-}C_5H_4COCH_3)Nb(CO)_4$			
a_1 (d_{z^2})	7.44	0.26	0.24	0.45	1.03	2.31
b_2 (d_{xy})	7.75	0.31	0.29			
Cp e_1''	9.50	0.48	0.31	1	1	1
	9.91s	0.50	0.45			
			$(\eta^5\text{-}C_5H_4SiMe_3)Nb(CO)_4$			
a_1 (d_{z^2})	7.27	0.29	0.27	0.71	2.12	2.98
b_2 (d_{xy})	7.52	0.29	0.22			
Cp e_1''	9.16	0.40	0.30	1	1	1
	9.56s	0.39	0.37			
Si−C	10.50	0.67	0.40	1.88	1.07	0.57
Si−C	11.04	0.70	0.70			
			$(\eta^5\text{-}C_5H_4SiMe_3)Ta(CO)_4$			
a_1 (d_{z^2})	7.27	0.35	0.25	0.76	2.03	2.67
b_2 (d_{xy})	7.51	0.23	0.20			
Cp e_1''	9.29	0.37	0.23	1	1	1
	9.69s	0.42	0.40			
Si−C	10.55	0.60	0.35	1.68	1.32	0.78
Si−C	11.05	0.71	0.60			

[a] s = shoulder.

in Figure 2. From the Fenske−Hall calculations these orbitals are 82% Cp e_1'' in character, 12% metal, and 6% carbonyl.

Metal−Carbonyl-Based Ionizations. Asymmetric Gaussian peaks are used to model the data in order to quantitatively represent each band profile in analytical form. The analytical representations of the ionizations of $CpV(CO)_4$, $CpNb(CO)_4$, and $CpTa(CO)_4$ are listed in Table 2 and illustrated in Figures 3 and 4 for the V and Ta molecules. The parameters listed in Table 2 are very similar for each molecule, providing quantitative support for the visual impression of the similarity between these spectra that was noted earlier. Five main points should be addressed with regard to the metal−carbonyl-based ionizations: the constancy of the ionization band positions, the similar relative area of band **I** from V to Nb to Ta in the He I spectra, the shoulder on the high-energy side of the ionization band, the broad ionization on the lower energy side of the first band, and the larger relative intensity of ionization band **I** compared to band **II** in the He II spectra. These features will be discussed in turn.

First, the positions of the ionizations in band **I** are the same within experimental error from the V to Nb to Ta molecules. Metal substitutions down a group in the periodic table are often used to identify the metal-based ionizations by the ionization energy shifts that are observed. For example, the difference in energy of the metal-based ionizations from $(\eta^6\text{-mesitylene})_2V$ to

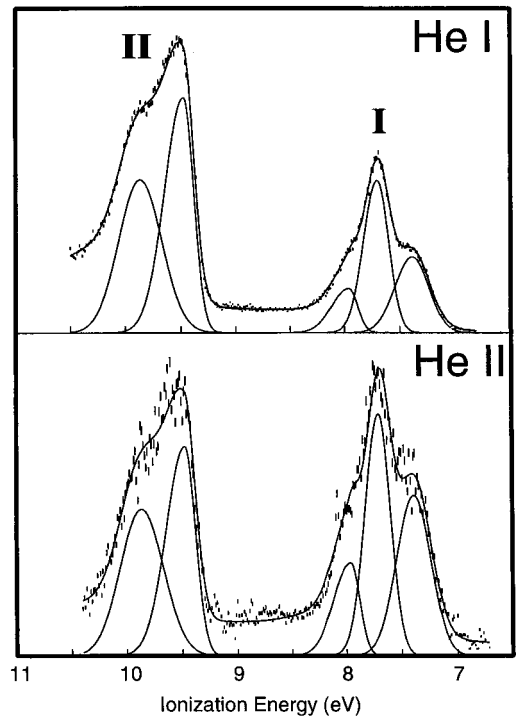

Figure 3. He I and He II close-up spectra of $(\eta^5\text{-}C_5H_5)V(CO)_4$.

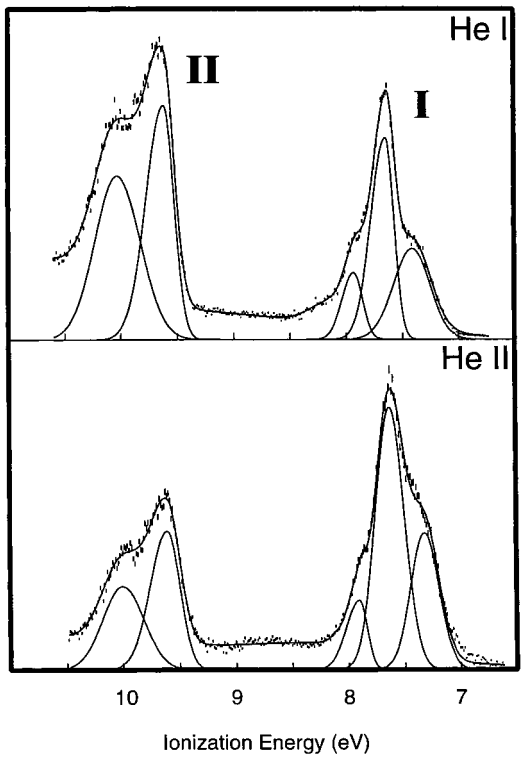

Figure 4. He I and He II close-up spectra of $(\eta^5\text{-}C_5H_5)Ta(CO)_4$.

$(\eta^6\text{-mesitylene})_2Nb$ is about 0.40 eV.[4] However, the difference in energy of the metal−carbonyl-based ionizations of $CpV(CO)_4$ and $CpNb(CO)_4$ found here is only 0.02 eV on average. Typically, when an ionization does not shift with substitution of an atom in a molecule, it signals that such an ionization arises from an orbital that has little character of that atom.

Second, the relative intensity of these predominantly metal−carbonyl-based ionizations looks to increase only

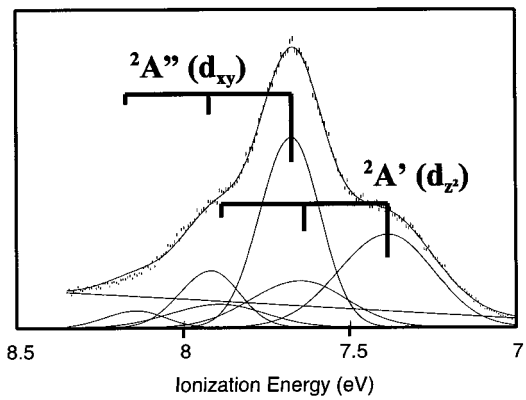

Figure 5. Simulation of vibrational progressions in the first ionization band of (η^5-C_5H_5)Nb(CO)$_4$.

slightly from V to Ta in the He I spectra. An increase is commonly observed in first- to third-row transition-metal comparisons and is a natural consequence of narrowing of the ionization bands due to the increased mass of the heavier metal. However, the areas of the metal−carbonyl-based ionization bands relative to the Cp-based ionization bands are almost the same from the V to Nb to Ta molecules. The relatively constant area is in contrast to the expectation of a large change in cross section between ionization of vanadium 3d electrons in comparison to ionization of niobium 4d and tantalum 5d electrons with He I excitation, as shown in Table 1. This is another indication that the formally d^4 metal density is extensively delocalized to the carbonyls.

Third, a strong C−O vibrational progression is observed on the high ionization energy side of band **I**. Progressions such as observed here have also been observed for other metal−carbonyl complexes and have been identified with the carbonyl stretching vibration.[31,32] The measured vibrational spacing on this band is 2000 ± 75 cm^{-1}, which agrees with the experimental symmetric carbonyl stretching frequency of 2029−2034 cm^{-1} for these molecules. This vibrational progression on the high binding energy side of the first band is particularly strong and is another result of the strong π back-bonding between the metal center and carbonyl ligands.

Fourth, a detailed examination of band **I** of CpNb(CO)$_4$ shown in Figure 5 indicates a relatively broad leading shoulder at lowest ionization energy and a sharper and more intense ionization component near the middle of the band, followed by the progression of ionizations, tailing off to higher binding energy. These different shapes of the leading shoulder and the intense central ionization indicate that these are two different electronic ion states. For reasons to be discussed shortly, the leading shoulder is assigned to the metal−carbonyl a_1 ionization and the intense central ionization is assigned to the metal−carbonyl b_2 ionization. Since both a_1 (d_{z^2}) and b_2 (d_{xy}) orbitals can back-bond to carbonyls, a C−O vibrational progression is expected to be associated with the a_1 ionization just as observed for the b_2 ionization, and this a_1 ionization progression will add intensity under the components of the b_2 ionization progression as shown in Figure 5. In this figure the ionization intensity is simulated by vibrational progressions with interval spacings of 2000 cm^{-1} on both the a_1 and b_2 ionizations (^{2}A′ and ^{2}A″ states of the positive ion, respectively). The heavy vertical lines represent the intensity to each component in the progressions, and the width of each peak in the simulation is held equal to that observed for the adiabatic transition. The simulation suggests that the vibrational progression is slightly stronger for the a_1 ionization. The integrated probabilities for the a_1 and b_2 ionizations are near 1:1 in this simulation despite the difference in intensity of the first two peaks. This is partly because of the different widths of the a_1 and b_2 ionizations. The close-up spectra from 6.5 to 8.5 eV of all of the molecules reveal that the Gaussian describing ionization from the a_1 orbital is consistently more broad than the ionization from the b_2 orbital (see Figures 3 and 4). This greater width of the a_1 ionization is a measure of a larger geometric distortion of the positive ion. This geometry distortion will be discussed along with the results of the theoretical calculations.

Fifth, the intensity of ionization band **I** relative to ionization band **II** increases substantially from He I to He II excitation in all cases. This change will be discussed following a more detailed consideration of the characteristics of ionization band **II**.

Cp-Based Ionizations. Although it is expected based on symmetry and the Fenske−Hall calculations that the two Cp e_1'' π orbitals are degenerate, the spectra in Figures 3 and 4 clearly show a shoulder on the high binding energy side of this ionization. This band profile has also been observed for CpM(CO)$_3$ (M = Mn, Re) and its methylated derivatives, and a few proposals were considered to explain the consistent splitting that is observed.[6] The carbon−hydrogen stretching vibrational progression was ruled out from the spectra of Cp*M(CO)$_3$ (Cp* = η^5-C_5Me_5), where the same splitting was observed. The possibility of autoionization can be eliminated because the He II spectrum contains the same splitting pattern. Another possibility is a static Jahn−Teller distortion. However, previous studies have shown that, with a static Jahn−Teller distortion, the intensity of the split ionizations is nearly the same,[33] while the shoulder on the Cp e_1''-based ionization is always less intense than the main component. A ground-state distortion of the coordinated Cp ring is a possibility for lower symmetry complexes, but the large splitting of 0.4 eV would not be possible with the high electronic symmetry, as indicated by the calculations on the molecules in the present study.

Depending on the energy of the vibrational mode and the stabilization energy provided by distortion of the geometry, the Jahn−Teller effect can be either static or dynamic.[34] If the energy of a Cp vibrational mode is comparable to the stabilization energy provided by Cp ring distortion, strong vibronic coupling can occur.[35] To further examine the reasonableness of a dynamic

(31) Hubbard, J. L.; Lichtenberger, D. L. *J. Am. Chem. Soc.* **1982**, *104*, 2132−2138.
(32) Wu, J.; Bancroft, G. M.; Puddephatt, R. J.; Hu, Y. F.; Li, X.; Tan, K. H. *Inorg. Chem.* **1999**, *38*, 4688−4695.
(33) Hubbard, J. L.; Lichtenberger, D. L. *J. Chem. Phys.* **1981**, *75*, 2560.
(34) Bersuker, I. B. *The Jahn−Teller Effect and Vibronic Interactions in Modern Chemistry*; Plenum Press: New York, 1984.
(35) Bahr, A.; Cooper, G.; Green, J. C.; Longley, K. A.; Lovell-Smith, M.; McGrady, G. S. *Chem. Phy.* **1996**, *203*, 223−231.

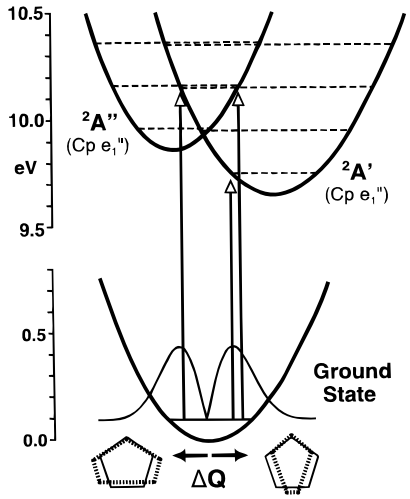

Figure 6. Potential well description of the dynamic Jahn−Teller effect in the Cp e_1'' π ionization of $CpNb(CO)_4$. The potential wells for the neutral ground state and the $^2A'$ and $^2A''$ (Cp e_1'') positive ion states are from ab initio calculations along the distortion coordinate. The distortion coordinate (see Experimental Section) is shown amplified by ±10 relative to a D_{5h} Cp ring.

Jahn−Teller effect in these systems, ab initio electronic structure calculations have been carried out to estimate the stabilization energy provided by Cp ring distortion. The details of these calculations are provided in the Experimental Section, and the results are illustrated in Figure 6. The potential wells of the positive ion states obtained from Cp e_1'' ionization of $CpNb(CO)_4$ are shown at the top of the figure. The calculations show that distortion of the Cp ring to local C_{2v} symmetry provides a stabilization energy of about 0.3 eV for the $^2A'$ (Cp e_1'') positive ion state and about 0.1 eV for the $^2A''$ (Cp e_1'') positive ion state. The Jahn−Teller active, doubly degenerate C−C stretching vibrational modes that correspond to this distortion have energies near 0.2 eV (1600 cm^{-1}). The similarity of the vibrational energy spacing to the stabilization of the positive ion states by distortion indicates the presence of a dynamic Jahn−Teller effect.

The observation that the splitting in the Cp e_1'' ionization is about 0.4 eV is suggested by the relationships between the potential wells and the vibrational levels in Figure 6. The potential energy of the ground state of the neutral molecule along the Cp distortion coordinate is shown at the bottom of Figure 6. Placed on the $\nu = 0$ vibrational level of the neutral molecule is the probability distribution for distortion Q from D_{5h} symmetry by a doubly degenerate, Jahn−Teller active vibrational mode. Remember that because this vibration is doubly degenerate, the probability for ionization from a molecule with perfect D_{5h} symmetry vanishes.[33] For the positive ions, the vibrational levels before vibronic coupling are approximated by the dashed lines. These levels will be shifted and split by the vibronic coupling. A full evaluation of the vibronic effects is beyond the scope of this study.[34] Also not included in Figure 6 are interactions between the $^2A'$ and $^2A''$ potential wells in the vicinity of their crossing at D_{5h} symmetry, which may also serve to diminish ionization intensity in the region of 0.2 eV above the initial Cp-based ionization. The classical description of ionization intensity is depicted by the vertical arrows in the diagram, which show that ionizations to the classical turning points of the potential wells will be split by about 0.4 eV. The splitting indicated by the calculations matches the observed 0.4 eV separation of the shoulder on this Cp-based ionization band.

Ionization from the e_{1g} π molecular orbitals of benzene shows a similar effect for similar reasons. The primary ionization is at 9.24 eV, and a "rather obscure structure" beyond 9.6 eV is observed which is attributed to Jahn−Teller splitting of the doubly degenerate electronic ground state of the cation.[36] The Jahn−Teller active E_{2g} vibrational mode of benzene has an energy of 0.196 eV, so the ionization intensity that is observed approximately 0.4 eV higher in energy than the lowest energy ionization is consistent with the dynamic Jahn−Teller effect.

He II Spectra. He II spectra help to reveal the atomic character of the orbitals corresponding to each ionization band.[37] As shown in Table 1, ionizations arising from primarily vanadium-based orbitals and oxygen-based orbitals are expected to increase in relative intensity compared to the ionizations arising from carbon-based orbitals when the photon source is switched from He I to He II. To illustrate, the close-up He I and He II spectra of $CpV(CO)_4$ from 6.5 to 11 eV are shown in Figure 3. The relative intensity of band **I** increases relative to band II, which supports the assignment of band **I** containing more metal d and/or oxygen character than band **II**.

The relative intensity changes in the He I and He II spectra of the Nb and Ta molecules, as shown in Table 2, provide an interesting comment on the metal or oxygen character in the first ionization band. According to theoretical estimates,[24] predominantly metal-based ionization bands for Ta should, unlike V, decrease in relative intensity from He I spectra to He II spectra. However, Table 2 shows an intensity increase of ionization band **I** for the Nb and Ta molecules that is greater than observed for the V molecule. Two factors must be contributing to this trend. First, the intensity of band **I** must have substantial oxygen character that results from the CO back-bonding. According to the theoretical prediction in Table 1, oxygen will increase its relative intensity almost double that of carbon. A large amount of oxygen character in the band ultimately pushes its relative intensity higher than in band **II**. Second, the Cp-based ionizations in band **II** must contain some metal character to account for the relative decrease of the intensity of band **II** with He II excitation for the Nb and Ta molecules. Using the cross sections in Table 1 to model the experimental trends in ionization probabilities in Table 2 suggests about 25% metal character in band **II** and predominantly oxygen character in band **I**. Precise determination of the characters is not possible because of approximations in calculating the theoretical atomic cross sections and because of limitations in the application of these atomic values to molecular systems, but these uncertainties are below the threshold of the general conclusions of substantial oxygen character associated with band **I** and partial metal character associated with band **II**.

(36) Turner, D. W.; Baker, C.; Baker, A. D.; Brundle, C. R. *Molecular Photoelectron Spectroscopy*; Wiley-Interscience: London, 1979.
(37) Green, J. C. *Acc. Chem. Res.* **1994**, *27*, 131.

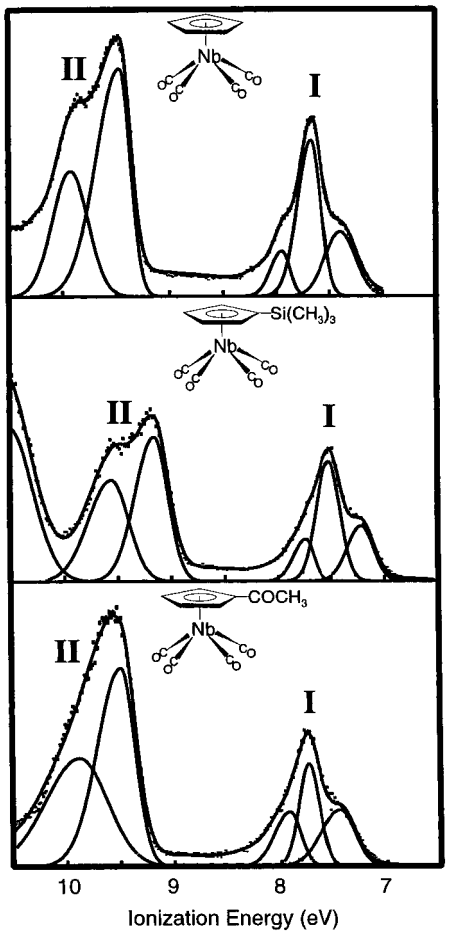

Figure 7. He I spectra of (η^5-C_5H_5)Nb(CO)$_4$, (η^5-C_5H_4-SiMe$_3$)Nb(CO)$_4$, and (η^5-C_5H_4COMe)Nb(CO)$_4$.

(η^5-C_5H_4R)M(CO)$_4$ (M = Nb, and Ta; R = trimethylsilyl; M = Nb, R=COCH$_3$). Photoelectron spectra of complexes with substituents on the Cp ring were collected to study the substitution effect. He I spectra of CpNb(CO)$_4$, (η^5-$C_5H_4SiMe_3$)Nb(CO)$_4$, and (η^5-C_5H_4COMe)-Nb(CO)$_4$ are shown in Figure 7. The photoelectron spectrum of (η^5-$C_5H_4SiMe_3$)Nb(CO)$_4$ shows a relatively small destabilization of the metal−carbonyl-based ionizations of about 0.15 eV, while the Cp-based ionizations are destabilized 0.32 eV. Similar results are found between tantalum and its substituted molecules. Because of the different electronic properties of the acetyl group, the shift of metal- and Cp-based ionizations is in the opposite direction of the trimethylsilyl substituent. The shifts of the metal−carbonyl-based ionizations upon substitution of Cp in these molecules contrasts to the systems such as ferrocene and (η^6-mesitylene)$_2$M molecules. For example, the difference of the predominantly metal-based ionizations between ferrocene and acetylferrocene is 0.30 eV,[38] while the difference of metal−carbonyl-based ionizations between (η^5-C_5H_5)Nb(CO)$_4$ and (η^5-C_5H_4COMe)Nb(CO)$_4$ found here is only 0.05 eV. Again, the extensive carbonyl character in the metal−carbonyl-based ionizations diminishes the effect of substitutional perturbations on the electronic structure.

Theoretical Results. Geometry optimizations of the neutral molecule and the low lying cation states using both density functional theory (ADF package) and ab initio (Gaussian 94 package) methods were carried out. Both methods give good agreement with the experimental structures, and only the ADF results on the geometries are presented in Table 3. The agreement in interatomic distances ranges from about 0.02 to 0.05 Å, except for the metal−Cp distance in the case of Ta, which is calculated about 0.1 Å too long. Cp rotation about the Cp(centroid)−M bond results in only small differences (∼0.002 eV in energy, ∼0.001 Å in bond distances, ∼0.1° in bond angles).

Table 3. Selected Average Distances (Å) and Angles (deg) of the Neutral Molecules and Cations of (η^5-C_5H_5)M(CO)$_4$ (M = V, Nb, Ta) Determined by Experiment and by Density Functional Theory Calculations

	neutral molecule experimental	neutral molecule calculated	^{2}A″ (d_{xy}) ion calculated	^{2}A′ (d_{z^2}) ion calculated
		(η^5-C_5H_5)V(CO)$_4$[b]		
M−C_{Cp}	2.28(1)	2.25(2)	2.26(1)	2.25(2)
M−CO	1.963(7)	1.911(2)	1.965(4)	1.965(2)
α[a]	120(2)°	119(1)°	118.9(7)°	112.0(7)°
		(η^5-C_5H_5)Nb(CO)$_4$[c]		
M−C_{Cp}	2.41(2)	2.45(2)	2.44(1)	2.43(2)
M−CO	2.09(1)	2.075(0)	2.129(1)	2.130(1)
α	122(2)°	121.6(3)°	121.1(4)°	113.5(4)°
		(η^5-C_5H_5)Ta(CO)$_4$[d]		
M−C_{Cp}	2.39(3)	2.49(2)	2.48(1)	2.46(2)
M−CO	2.08(1)	2.108(4)	2.161(2)	2.162(4)
α	122(1)°	122(1)°	122(1)°	113(1)°

[a] α is the Cp(centroid)−M−CO angle. [b] Experimental values from gas-phase electron diffraction.[29] [c] Experimental values averaged from crystal structures of five Nb molecules with different substituents on Cp.[1,2,28] [d] Experimental values averaged from crystal structures of four Ta molecules with different substituents on Cp.[1,2]

The characters of the orbitals in the ADF calculations are very similar to the characters obtained from the Fenske−Hall calculations. The a_1 (d_{z^2}) orbital in the neutral Nb molecule is calculated to be 49% metal, 50% carbonyl, and 1% Cp. The b_2 (d_{xy}) orbital in the neutral molecule is calculated to be 48% metal, 50% carbonyl, and 2% Cp. The Cp e_1″-based orbitals are calculated to be 80% Cp, 12% metal, and 8% carbonyl. It is also noted that the cation states ^{2}A′ (d_{z^2}) and ^{2}A″ (d_{xy}) reveal an increase of the metal−carbonyl distance (∼0.05 Å) and a shortened carbon−oxygen distance (∼0.02 Å). These results are consistent with removal of electron density that is back-bonding to the carbonyl π^* orbitals.

The most significant result is the Cp(centroid)−M−CO angle α, which optimized at the experimental values in all cases. The total energy varies greatly with the change of the Cp(centroid)−Nb−CO angle α, which indicates the influence of the metal−carbonyl interaction on the molecular geometry. Figure 8 shows the density functional results for the energies of the top four orbitals as a function of the Cp(centroid)−Nb−CO angle α. The HOMO becomes less stable as the Cp(centroid)−Nb−CO angle α decreases, while the SHOMO varies only slightly. This is in agreement with the assignment of the HOMO as a_1 (d_{z^2}) and the SHOMO as b_2 (d_{xy}) due to their different back-bonding and σ bonding abilities with the carbonyls when the Cp(centroid)−Nb−CO angle α changes. Not only can the d_{z^2} orbital be π back-bonding to the carbonyls but the torus of d_{z^2} can also

(38) Fan, H.-J. Dissertation, University of Arizona, Tucson, AZ 85721, 1999.

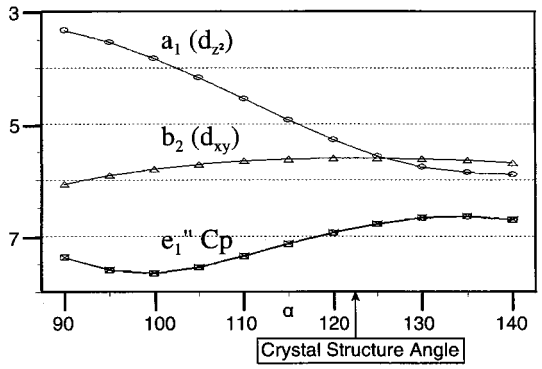

Figure 8. Trends in valence orbital energies with Cp(centroid)−Nb−CO angle α.

Table 4. Comparison of Ionization Energies (eV) by Various Methods with Experimental Values for (η^5-C_5H_5)Nb(CO)$_4$

cation state	orbital label	exptl IE	FH[a]	DFT	UHF	MP2
$^2A'$	a_1 (d_{z^2})	7.39	7.21	7.88	6.14	6.81
$^2A''$	b_2 (d_{xy})	7.67	7.74	8.00	6.46	7.74
$^2A'$, $^2A''$	Cp e_1''	9.46 (9.93s)	9.68, 9.69	9.40, 9.40	*b*	*b*

[a] Fenske−Hall orbital eigenvalues scaled by 0.8. [b] Calculations starting from these excited cation $^2A'$ and $^2A''$ states corresponding to removal of an electron from a Cp-based orbital collapse to the corresponding cation ground states of these symmetries.

have a metal−carbonyl σ overlap interaction as the angle α becomes smaller. In this case the σ overlap would lead to a filled−filled destabilizing interaction between the carbonyl σ donor orbital and the filled d_{z^2} orbital. The d_{xy} orbital can only have π back-bonding interaction with the carbonyls because the carbonyls remain in the nodal planes of the d_{xy} orbital as the angle α varies. When the angle α decreases from around 125°, the Cp e_1'' orbitals become more stable due to the better bonding with the metal as a consequence of less competition with carbonyl σ donor orbitals for donation into the metal d_{xz} and d_{yz} orbitals. The optimum geometry of the molecule is a balance of these factors.

On the basis of this diagram, it is expected that when an electron is removed from the highest occupied molecular orbital, the angle α should decrease. The optimized geometries of the cations indicate about an 8° decrease of Cp(centroid)−M−CO angle with ionization from the a_1 (d_{z^2}) orbital to produce the $^2A'$ cation state. A similar change was not found for ionization from the b_2 (d_{xy}) orbital to produce the $^2A''$ cation state. As pointed out early in the discussion, the broadening of the first metal−carbonyl-based ionization in the photoelectron spectra is probably due to a substantial geometry change upon ionization. The a_1 (d_{z^2}) ionization energy is more sensitive to distortion along this coordinate and gives rise to a larger geometrical relaxation, consistent with the a_1 (d_{z^2}) ionization being slightly broader than the b_2 (d_{xy}) ionization.

The ionization energies predicted by various computational methods are compared with the experimental values of CpNb(CO)$_4$ in Table 4. The orbital energies predicted by the Fenske−Hall method are scaled by a factor of 0.80, as mentioned earlier. The ionization energies from the ADF, ab initio Hartree−Fock, and MP2 calculations are obtained using the unrestricted ΔSCF procedure.[39,40] As shown in the table, all of the methods predict the splitting of two metal−carbonyl-based ionizations with the ionization from the a_1 (d_{z^2}) orbital to produce the $^2A'$ cation state occurring first. The electron relaxation energy associated with the first ionization energy of the Nb molecule is calculated to be in the range 1.5−2 eV, which is considerably less than the electron relaxation energy found for metal-based ionizations of organometallic molecules with metals to the right of Nb in the periodic table.[30] These electron relaxation energies are the subject of a separate investigation.[38] Fenske−Hall and ADF results show that the Cp-based orbitals and ionizations are essentially degenerate before distortion of the molecules.

Comments and Conclusions

These molecules show interesting geometry changes with ionization. A geometry change is found upon ionization of the orbital containing d_{z^2} character, as shown by the broadening of the lowest ionization energy band in the photoelectron spectra. Both density functional and ab initio calculations not only reproduce the neutral geometries satisfactorily, compared with both gas-phase electron diffraction and crystal structure data, but also support a geometry change upon the ionization with metal d_{z^2} character. This change may be important to the reaction chemistry of these molecules, as it opens the site symmetrically between the four carbonyls as the molecules are oxidized. The photoelectron spectra also reveal the consistent splitting of the Cp-based ionizations, which follows from a Jahn−Teller distortion coupled dynamically with a degenerate Cp C−C vibrational stretching mode.

These photoelectron spectroscopic studies on CpM(CO)$_4$ (M = V, Nb, Ta) reveal that the strong delocalization of electron density from the metal to the carbonyl ligands dominates the electronic structure of this class of molecules. Several observations are found in support of the strong interactions: the lack of shift with metal substitution of the ionizations that arise from the formal d^4 configuration; the strong C−O vibrational progressions on the high binding energy side of the predominantly metal−carbonyl-based ionization band; the similarity of the ionization intensities from vanadium to tantalum; and the small perturbation effect upon functionalization of the Cp ring. Both the Fenske−Hall and ADF calculations predict about 50% of carbonyl ligand character is mixed into the first two metal orbitals in the neutral molecules. The experiments suggest even greater carbonyl character associated with these ionizations.

The delocalization of the metal electron density to the carbonyls appears to be exceptionally strong in these molecules in comparison with that in other metal−carbonyl molecules. Several factors likely contribute to this observation. First, the d orbitals of the early transition metals are inherently less stable and more spatially diffuse than those of later transition metals, favoring good energy match and overlap with the carbonyl π^* orbitals for electron donation from the metal. Second, the carbonyls are not competing with

(39) Bagus, P. S. *Phys. Rev. Sect. A* **1965**, *139*, 619.
(40) Moser, C. M.; Nesbet, R. K.; Verhaegen, G. *Chem. Phys. Lett.* **1971**, *12*, 230.

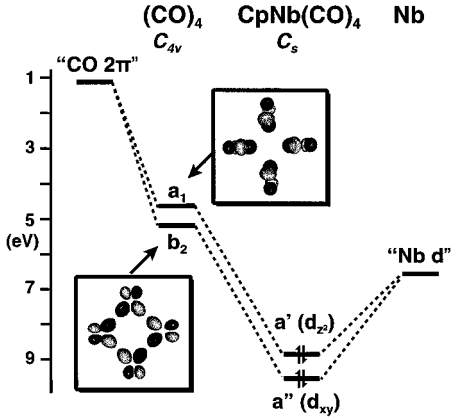

Figure 9. Molecular orbital diagram of (η^5-C_5H_5)Nb(CO)$_4$ constructed from a Fenske−Hall calculation in terms of the a_1 and b_2 group orbitals of the four carbonyls. The a_1 and b_2 group orbitals of $(CO)_4$ are viewed down the 4-fold symmetry axis from the location of the metal to the center of the carbonyls.

other strong π acceptor ligands which may withdraw electron density and stabilize the metal. The cyclopentadienyl ligand bonds primarily as a donor to the empty metal d orbitals and is only a weak acceptor that does not compete well for electron density from the d_{xy} orbital or from the d_{z^2} orbital. Third, each occupied metal d orbital donates to four carbonyls. Furthermore, the symmetry combinations of the four carbonyl π acceptor orbitals that overlap with the metal d orbitals are bonding between the carbonyls, and this interligand bonding character provides additional stabilization to these group orbitals and greater propensity for these orbitals to accept electron density.

The importance of this latter point is illustrated in the molecular orbital diagram of $CpNb(CO)_4$ in Figure 9 . This diagram focuses on the interaction of the metal d orbitals with the appropriate $(CO)_4$ group orbitals. The nodal properties of the orbitals make the overlap interactions clear. Pictured in the diagram are the a_1 and b_2 combinations of the 2π orbitals of the four carbonyls oriented as in the molecular geometry. It can be seen that the a_1 combination of the $(CO)_4$ 2π orbitals is bonding between the carbonyls and is substantially stabilized in comparison with a single carbonyl 2π orbital, which has the energy shown on the left of the diagram. The same occurs for the b_2 combination of the carbonyl 2π orbitals. This interligand interaction is especially significant in this class of molecules because the near 120° angle of the carbonyls from the 4-fold axis moves the four carbonyls closer to each other. The bonding stabilization of the carbonyl a_1 and b_2 π orbitals moves these orbitals to energies that are comparable with the metal d orbitals. The $(CO)_4$ a_1 group orbital overlaps well with the metal d_{z^2} orbital, and the small energy gap between these orbitals leads to a molecular orbital that is almost evenly distributed between the metal and the carbonyls in these calculations. The $(CO)_4$ b_2 group orbital overlaps well with the metal d_{xy} orbital, and this interaction leads to a similar result. The slightly smaller stabilization of the $(CO)_4$ a_1 orbital compared to the b_2 orbital is due to the poorer interligand overlap in the a_1 symmetry combination, and this in turn results in a smaller stabilization of the a_1 (d_{z^2}) orbital compared to the b_2 (d_{xy}) orbital. It is interesting that the electron donation from the metal to the carbonyls that strengthens the M−CO bonding also leads to interligand bonding between the carbonyls. The general conclusion is that although these molecules are formally considered to have d^4 metal configurations, the spectroscopy and the calculations show that this electron density is substantially distributed to the carbonyls.

Acknowledgment. D.L.L. acknowledges the support by the U.S. Department of Energy (Division of Chemical Science, Office of Basic Energy Sciences, Office of Energy Research, DE-FG03-95ER14574), the National Science Foundation, (Grant No. CHE-9618900), and the Materials Characterization Program, Department of Chemistry, the University of Arizona.

OM990921M